Steric Trigger as a Mechanism for CB_1 Cannabinoid Receptor Activation

Joong-Youn Shim* and Allyn C. Howlett

Julius L. Chambers Biomedical/Biotechnology Research Institute, North Carolina Central University, Durham, North Carolina 27707

Received January 16, 2004

To determine the moiety that behaves as the steric trigger to activate the CB_1 cannabinoid receptor, conformational properties of the nonclassical cannabinoid CP55244, one of the most potent CB_1 receptor agonists, were characterized by conformational analysis, rotational barrier calculations, and molecular dynamics (MD) simulations. It was shown from the present MD simulations that the torsion angles $\varphi 1$ and $\varphi 4$ of the C3 side chain showed the most dramatic change when compared with the ground-state receptor-bound conformation, indicating that rotation around these torsion angles is responsible for releasing the ligand strain energy. Multiple stages would be involved in the ligand conformational change. As a molecular mechanism for the ligand-induced CB_1 receptor conformational change, we propose that the C3 side chain serves as the steric trigger, while the ACD-ring moiety of CP55244 serves as the plug. Steric clash with helices within the binding pocket would induce microconformational adaptation within the protein. This mechanism would suggest that rotational flexibility in a ligand may be as important a determinant of agonist activity as the pharmacophoric elements that can be identified.

INTRODUCTION

G-protein coupled receptors (GPCRs), composed of seven transmembrane (TM) helices,[1,2] are known to be among the most important drug targets.[3] GPCRs are classified into three families: class I (A) rhodopsin-like; class II (B) secretin receptor-like; and class III (C) metabotropic glutamate-receptor-like.[2] Despite the overall low sequence homology,[4] highly conserved amino acid residues in the TM helical domains of GPCRs are indicative of common structure or functions of GPCRs.[5−7] In response to ligand binding, GPCRs change their conformations to activate the associated G-proteins.[2,7] Two receptor models for describing the ligand-mediated G-protein activation have been proposed: the conformational selection model and the ligand induction model (for a review, see ref 2). In the conformational selection model,[8,9] agonists preferentially bind to the receptor in the R* (active) conformation over the receptor in R (ground) conformation, thereby increasing the duration of time that the receptor remains in the R* state. In contrast, according to the ligand induction model,[10,11] ligands initially bind to the R state and induce a conformational change to the R* state. The conformational selection model is appropriate for protein monomers or multimers in which cooperative interactions are readily reversible between two interconvertible states. A problem in applying the conformational selection model to GPCRs is that the activation process by which the receptor-G-protein complex releases GDP from the Gα subunit can only occur as the result of a conformational change in the proteins.[12,13] That state is not readily reversible after the elimination of GDP from its binding site. In the presence of GTP or an analogue, GTP would occupy that site, conferring an additional conformational change(s) in the receptor-G-protein complex that results in dissociation of the proteins. Under these cellular or experimental conditions, the receptor assumes a state of low affinity for the agonist ligand, such that release of the ligand is facilitated. The activation cycle is terminated when the Gα protein hydrolyzes the GTP to GDP and reassociates with the $\beta\gamma$ dimer and the receptor. The receptor-G-protein heterotrimer complex assumes a state of high affinity for the agonist ligand such that the activation cycle can be reinitiated by the binding of an agonist. This cycle of conformational changes is driven by the agonist's interaction with the receptor and GTP's interaction with the Gα protein. This sequence of conformational changes is monitored experimentally as a sequence of negative heterotropic interactions in which GTP plus a G-protein trimer reduces the receptor's affinity for the agonist, and the agonist plus receptor reduces the G-protein's affinity for GDP.

Recent studies on rhodopsin[14,15] and the β_2 adrenergic receptor[11,16] suggested agonist-induced rigid-body TM helical displacement as a mechanism for the conformational change associated with receptor activation. The molecular mechanism for activation of rhodopsin is predicated upon the ligand acting as the steric trigger for the conformational change.[17−22] This conformational trigger mechanism is based on biochemical and structural data that describe a sequence of protein structural modalities (for reviews, see refs 23 and 24). First, the ligand retinal is covalently bound to residue K7.43(296) in TM7 as its protonated Schiff base. The ligand, then, is isomerized from the 11-*cis* to the all-*trans* form by the energy of light.[25,26] The movement of the β-ionone ring moiety of retinal toward TM3 and TM4 causes a significant steric repulsion to TM3, leading to the rearrangement of the surrounding helices, TM6 and TM7. The rhodopsin conformational change in response to the retinal conformational trigger promotes G-protein activation (i.e., GDP release).

* Corresponding author phone: (919)530-7015; fax: (919)530-7760; e-mail: jyshim@wpo.nccu.edu.

10.1021/ci040040c CCC: $27.50
Published on Web 07/01/2004

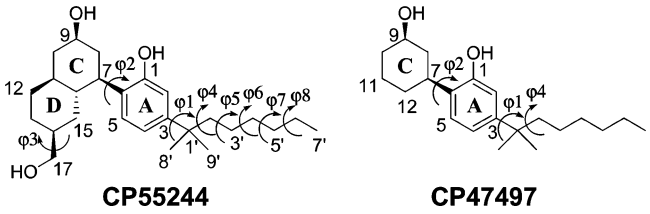

Figure 1. Molecular structures of the CB_1 receptor nonclassical cannabinoid agonist ligands, defining the torsion angles, φ1(C2−C3−C1′-C2′), φ2(C1−C6−C7−C16), φ3(C13−C14−C17−O), φ4(C3−C1′-C2′-C3′), φ5(C1′-C2′-C3′-C4′), φ6(C2′-C3′-C4′-C5′), φ7(C3′-C4′-C5′-C6′), and φ8(C4′-C5′-C6′-C7′), analyzed in this study.

The concept of the steric trigger for rhodopsin's conformational change can be applied to GPCR's responding to diffusible ligands. These receptor systems are characterized by properties that differ from the rhodopsin system: (1) Unlike retinal's association with rhodopsin, the diffusible receptor ligands are unable to form a covalent bond with the receptor to function as the attachment site. Therefore, diffusible ligands must possess a moiety or moieties that can form a sufficiently strong interaction with the receptor to position the ligand securely in its active site. This moiety could be referred to as the "plug". (2) Unlike photoactivation in rhodopsin, no external energy source drives the ligand conformational change for releasing internal structural strain. Therefore, for receptor conformational changes induced by nonactivated ligands, it is necessary for the ligand to provide a steric trigger mechanism based upon a source of internal energy within the ligand itself. This could be provided by the release of internal structural strain imposed upon the ligand as it adapted to the binding pocket of the receptor in the R state (ground state).

Brain CB_1 cannabinoid receptors are GPCRs[27,28] and belong to the rhodopsin-like subfamily,[2] suggesting a similar molecular mechanism for G-protein activation as for rhodopsin. To determine the mechanism for the steric trigger in the CB_1 receptor system, conformational properties of the nonclassical cannabinoid agonist CP55244 were characterized by conformational analysis, rotational barrier calculations, and molecular dynamics (MD) simulations. Analysis of binding conformations[29] that achieve low free energy states after release from the ground-state conditions led us to postulate that the C3 side chain of the nonclassical cannabinoids serves as the steric trigger and the ligand strain energy as the trigger mechanism for the CB_1 receptor conformational change leading to G-protein activation.

COMPUTATIONAL METHODS

All the calculations were performed on a Silicon Graphics Origin2000 workstation. Low energy conformations of CP55244 were determined by a Monte Carlo (MC) search involving a simulated annealing by heating the system up to 5000 K and a systematic search using the molecular mechanics MMFF94 force field[30] implemented in Spartan'02 (Wavefunction, Inc. Irvine, CA). For the systematic conformational searches, all the rotatable torsion angles (see Figure 1 for the definition of the torsion angles) were systematically searched by a 3-fold rotation, with the exceptions of φ1, for which a 6-fold rotation was used, and φ2, for which a 2-fold rotation was used.

Rotational energy barrier calculations were performed using the molecular mechanics MMFF94, semiempirical AM1,[31] ab initio HF/3-21G(*),[32] and density functional[33] B3LYP/6-31G* methods implemented in Spartan'02, using the lowest energy conformation of CP55244 from the conformational search. For the MMFF94 and AM1 calculations, all the structural elements were fully optimized except the torsion angle selected as the torsional driver. For the HF/3-21G(*) and B3LYP/6-31G* calculations, a single point energy at the MMFF-optimized geometries was calculated. A torsion angle driver was taken in 10° increments for the range of 360° (i.e., 36 increments) as the function of the individual torsion angles, φ1 through φ8 (Figure 1).

MD simulations were performed using MMFF94 implemented in SYBYL (version 6.8) (Tripos, Inc., St. Louis, MO). After extracting the ligand from the complex structure within the CB_1 receptor binding pocket[29] (defined as the receptor in its ground state, see below), this binding conformation of CP55244 was subjected to a MD simulation (NVT, canonical ensemble) of 35 ns at 300 K. Because the CB_1 receptor binding pocket seemed to be located within the hydrophobic core[29,34] formed by the TM helical domains, an implicit solvation model with a distance-dependent dielectric constant of 4 ($\epsilon = 4r$) was used. The nonbonded lists were generated using a 12 Å nonbonded cutoff distance and updated every 25 fs. The temperature was controlled by direct scaling of velocities, and the equations of motion were integrated by the Verlet velocity method.[35,36] Thirty-five thousand structures were extracted from the trajectories by sampling every 1 ps. These structures were used to analyze and characterize the individual torsion angles, φ1 through φ8 (Figure 1).

RESULTS

In a previous study,[29] the CB_1 receptor homology model was developed from the X-ray crystal structure of rhodopsin with retinal in the 11-*cis* conformation. This conformation would represent the ground state for the receptor structure. The CB_1 agonist CP55244 was docked into the CB_1 receptor with the receptor held rigidly in the ground state in such a way as to minimize the free energy of the ground-state ligand−receptor (LR) association. However, this conformation of the ligand does not represent the lowest free energy state of that molecule as it might exist in a completely unconstrained environment. To explore the mechanism by which the ligand can seek and attain its lowest state from its initially constrained conformation, we isolated the ligand in the conformation that was identified in the constrained, ground-state LR form. We then examined each torsion angle in order to determine the relative probability of movement, given thermodynamic barriers to rotation.

Rotational Barrier Energy Calculations on CP55244. Rotational barrier energies for CP55244 were estimated by torsional driver calculations, using MMFF94, AM1, *ab intio* HF/3-21G(*), and density functional B3LYP/6-31G* methods. The rotational energy barriers calculated for CP55244 are represented in Figure 2. All the calculation methods showed similar energy profiles, although the AM1 method appeared to underestimate the energy barriers when compared with the other methods. Rotations around φ1 and φ3 showed very low energy barriers (<5 kcal/mol), indicating that

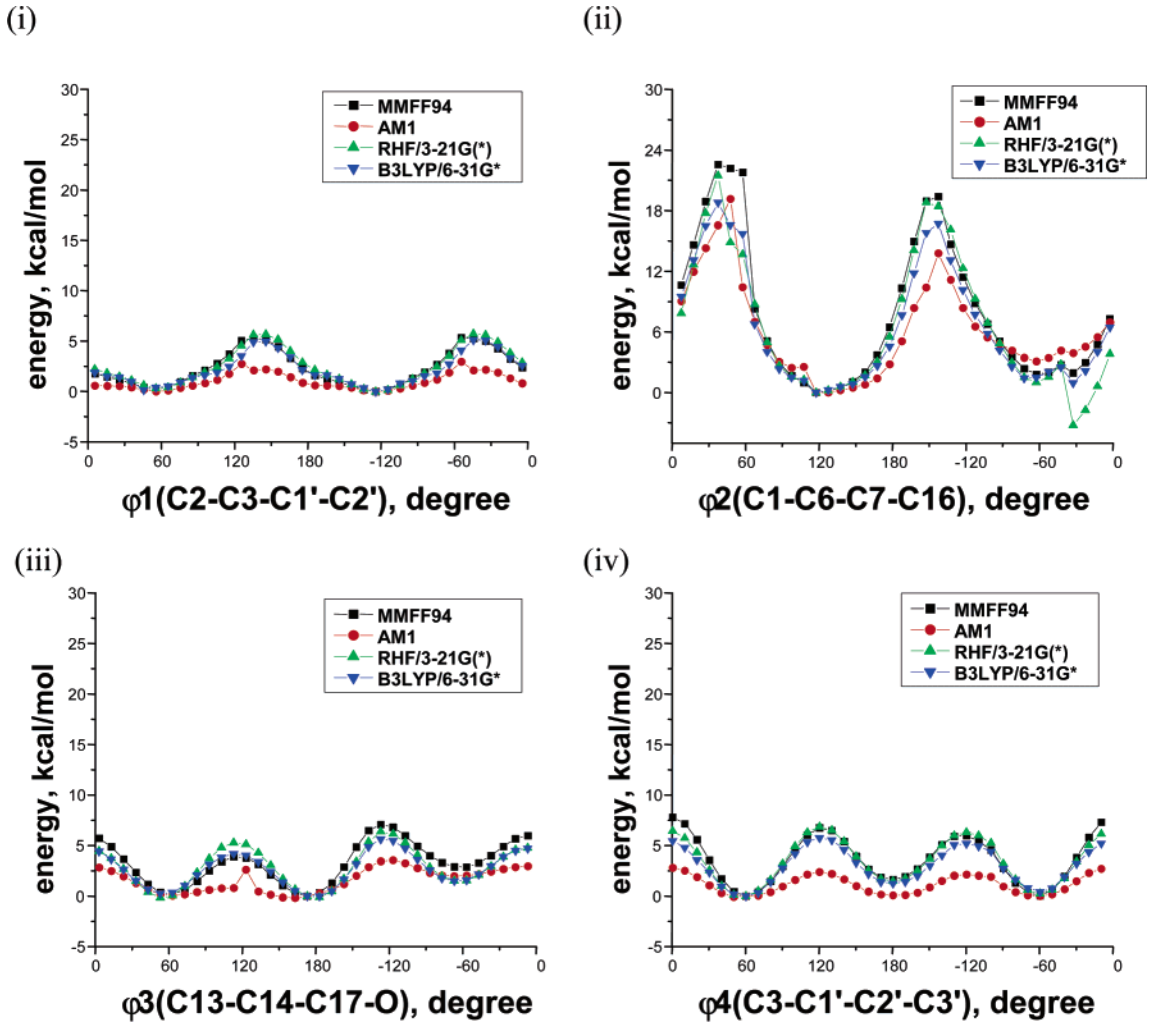

Figure 2. MMFF94, AM1, RHF/3-21G(*), and B3LYP/6-31G*-derived rotational energy barriers (in kcal/mol) of CP55244 calculated for (i) $\varphi 1$, (ii) $\varphi 2$, (iii) $\varphi 3$, and (iv) $\varphi 4$.

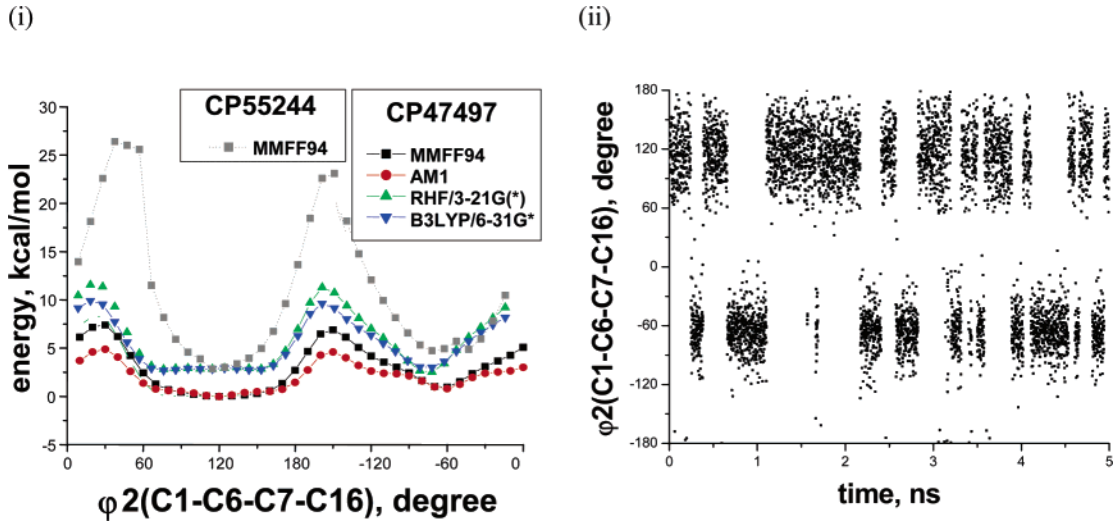

Figure 3. (i) MMFF94, AM1, RHF/3-21G(*), and B3LYP/6-31G*-derived rotational energy barriers (in kcal/mol) of CP47497 in comparison with CP55244 calculated for $\varphi 2$. (ii) Conformational preference of CP47497 calculated for $\varphi 2$ during a 5 ns MD simulation at 300 K.

rotations around these torsion angles might be freely accessible at physiological temperatures. In contrast, rotation around $\varphi 2$ showed two high-energy rotational barriers at $\varphi 2 = 38°$ (>16 kcal/mol) and at $\varphi 2 = -142°$ (> 14 kcal/mol), where the A-ring becomes parallel to the C-ring. Rotational barriers around $\varphi 2$ are high due to the presence of the sterically bulky D-ring, which hinders the rotation of the C/D-ring moiety and leads to a limited capability of rotation.

Rotational barrier energies for CP47497 were also estimated. As shown in Figure 3(i), $\varphi 2$ of CP47497 showed significantly decreased (about 10−12 kcal/mol) rotational energy barriers when compared with CP55244; the barrier

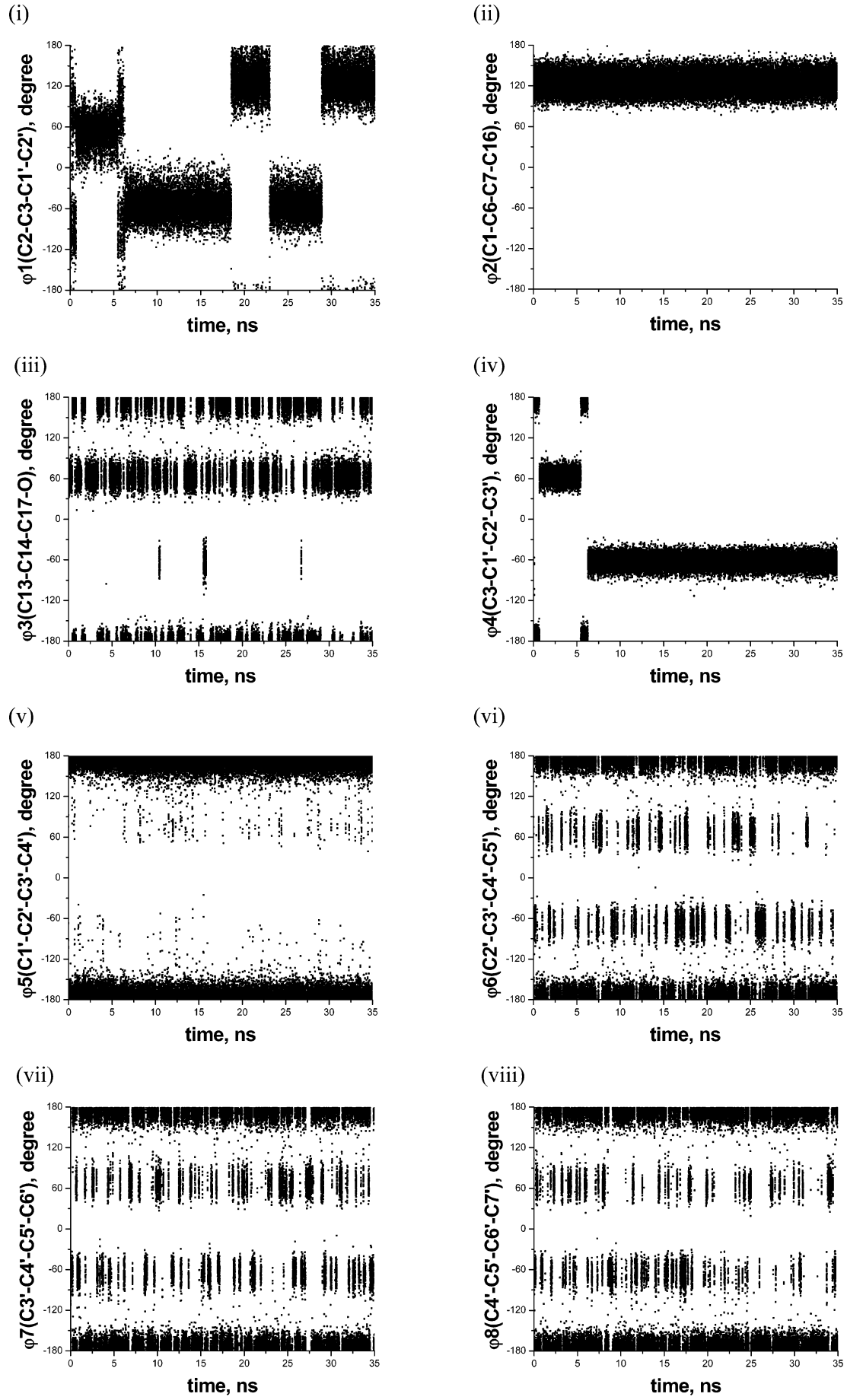

Figure 4. Conformational preference of CP55244 calculated for the individual torsion angles, (i) $\varphi 1$, (ii) $\varphi 2$, (iii) $\varphi 3$, (iv) $\varphi 4$, (v) $\varphi 5$, (vi) $\varphi 6$, (vii) $\varphi 7$, and (viii) $\varphi 8$, during a 35 ns MD simulation at 300 K.

was estimated to be 4−8 kcal/mol. Rotations around $\varphi 4$ of CP47497 also showed relatively low energy barriers (<7 kcal/mol) (data not shown).

MD Simulations of CP55244 as It Relaxes from Its Ground-State Receptor-Bound Conformation. All eight rotatable torsion angles, $\varphi 1-\varphi 8$, were analyzed by 35 ns MD simulation at 300 K (Figure 4). The MD plot showed that $\varphi 1$ remained within the low energy trough around 60° for about 5 ns. After a very short transitional period (<1 ns), the molecule overcame the low rotational barrier of $\varphi 1$, and the angle value converged to around −60°. For the remainder of the 35 ns MD simulation, the $\varphi 1$ angle flip-flopped between −60° and 120° angle values. $\varphi 4$ preferred the torsion angle value of 60° or −60° (i.e., the *gauche* forms) over 180° (i.e., the *anti* from). This is consistent with the troughs located at these regions of the rotational energy profile [Figure 2(iv)]. It was shown from the MD simulation that $\varphi 5$ had a strong preference for the *anti* over the *gauche* form (*anti/gauche* ratio ~ 77.1/1), whereas the torsion angles at the end of the C3 side chain, $\varphi 6$ (*anti/gauche* ratio ~ 2.4/1), $\varphi 7$ (*anti/gauche* ratio ~ 2.1/1), and $\varphi 8$ (*anti/gauche* ratio ~ 3.2/1) showed great versatility in their conformational geometries.

Throughout the entire MD simulation, the value of $\varphi 2$ remained unchanged around 120° as it existed in the initial ground-state receptor-bound conformation. This result suggests that the orientation of the A-ring with respect to the decaline CD-ring moiety would not deviate due to the high energy barriers that must be overcome in order to do so. Thus, the ACD-ring moiety of CP55244 would be expected to remain as a rigid unit within the receptor binding region without being distorted during receptor conformational changes. It was shown from the present simulation that $\varphi 3$ preferred the angle of 60° or 180° over −60°. These results were in agreement with the prediction based upon the energy profile from the rotational barrier calculations [Figure 2(iii)].

From the 35 ns MD simulation plot of CP55244, it can be seen that $\varphi 1$ and $\varphi 4$ of CP55244 showed the most dramatic changes when compared with the ground-state receptor-bound conformation. This indicates that rotation around these torsion angles is responsible for releasing the ligand internal strain energy. Interestingly, changes in $\varphi 1$ and $\varphi 4$ appeared to be closely associated with each other [Figure 4(i),(iv)]. The present MD trajectories of CP55244 suggest that multiple stages would be involved in the ligand conformational change (Figure 5): (1) starting from the ligand bound to the receptor in the ground-state conformation (**STATE_1**: $\varphi 1 = 114°$, $\varphi 4 = 173°$); (2) $\varphi 1$ changes to 56°, concurrent with a change of $\varphi 4$ to 61° to the lowest energy surface by passing a small energy barrier [Figure 2(iv)] (**STATE_2**: $\varphi 1 = 56°$, $\varphi 4 = 61°$). At this angle of $\varphi 1$, it is not possible for $\varphi 4$ to adopt −60° due to the steric repulsion between the A-ring and the C3 side chain (Figure 5); (3) $\varphi 1$ changes to −56°, concurrent with a change of $\varphi 4$ to −61° to the lowest energy surface by passing a 5−7 kcal/mol energy barrier [Figure 2(iv)] (**STATE_3**: $\varphi 1 = -56°$, $\varphi 4 = -61°$); and (4) $\varphi 1$ changes to 120°, with retention of $\varphi 4$ to −61° (**STATE_4**: $\varphi 1 = 124°$, $\varphi 4 = -61°$). **STATE_4** appears to be able to flip-flop with **STATE_3** with equal probability of occurrence in the later stage of the simulation [Figure 4(i)]. A detailed examination showed that the rotational energy barrier of $\varphi 1$ was governed by the torsion angle value of $\varphi 4$ (Figure 6). In other words, the rotational energy profile of $\varphi 1$ changed in association with $\varphi 4$. $\varphi 1$ showed virtually no energy barriers with the torsion angle value of $\varphi 4$ as found in **STATE_1**, where the $\varphi 4$ value is ~180°. However, it showed a distinct energy profile with troughs at 60° and −120° at **STATE_2**, where the $\varphi 4$ value is ~60° and, in turn, becomes shifted to the right about 60° to show troughs at 120° and −60° at **STATE_3**, where the $\varphi 4$ value is ~ −60°.

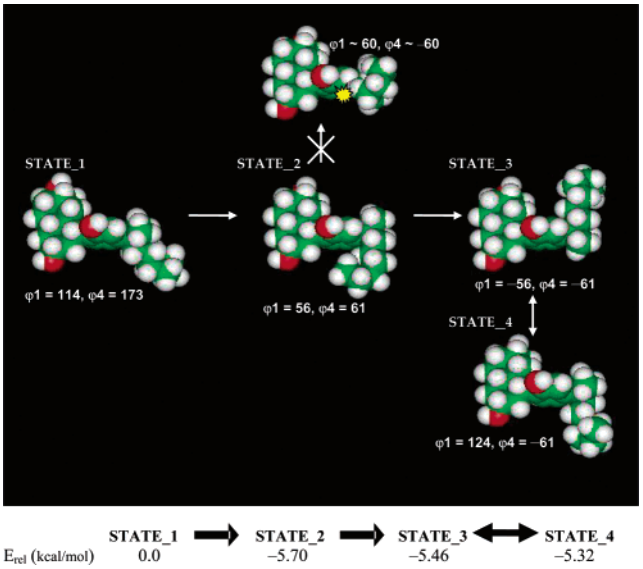

Figure 5. Conformational changes of CP55244 (in space-filling depiction) calculated for a combination of $\varphi 1$ and $\varphi 4$ during the 35 ns MD simulation at 300 K. Starting from the ground-state receptor-bound conformation (**STATE_1**), three low energy conformations (**STATE_2**, **STATE_3**, and **STATE_4**) were identified. An energetically unfavorable conformation with $\varphi 1 \sim 60°$ and $\varphi 4 \sim -60°$ is also depicted: the sterically unfavorable region is yellow starburst. Color coding of CP55244: green, C; red, O; and white, H.

To focus on the effects by the torsion angles $\varphi 1$ and $\varphi 4$, in this scheme of the multiple conformational stages, other torsion angles are assumed to be unchanged. The strain-free, low energy ligand conformations **STATE_2**, **STATE_3**, and **STATE_4** identified from the MD trajectories would be the most highly probable conformations to which the receptor would be subjected when the bound ligand tends to release its internal steric energy.

Overall, it is demonstrated that a series of sequential torsion angle changes orchestrated by the 'flexible' $\varphi 1$ and the associated $\varphi 4$ can induce a conformational change in the C3 side chain orientation of CP55244. Our MD simulation showing the key role of $\varphi 1$ and $\varphi 4$ is in agreement with the observation that $\varphi 1$ of classical and nonclassical cannabinoid agonists, connecting the A-ring and the C3 side chain, must be highly flexible to retain the agonist activity.[37,38]

The MD simulations for CP47497 torsion angles showed very similar results as described for CP55244, with the exception of $\varphi 2$. As predicted from the lowered rotational energy barrier for $\varphi 2$ in CP47497 due to the absence of the bulky D-ring [Figure 3(i)], the MD simulation of CP47497 showed that a noticeable population existed with $\varphi 2$ at −60° and 120° [Figure 3(ii)]. It is likely that this mobility around $\varphi 2$ in CP47497 could contribute to the observed decrease in binding affinity as well as a possible reduction in efficacy

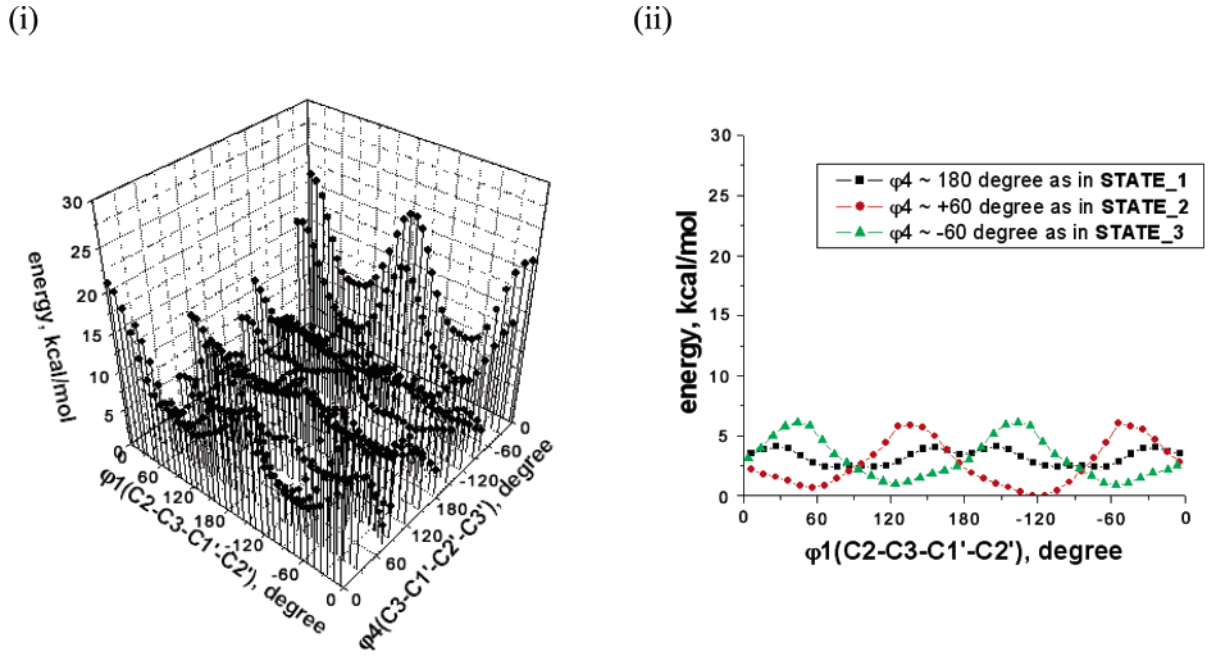

Figure 6. MMFF94-derived rotational energy barriers (in kcal/mol) of CP55244 calculated for a combination of $\varphi 1$ and $\varphi 4$. The torsional drivers for $\varphi 1$ and $\varphi 4$ were taken in 10° and 30° increments for the range of 360°, respectively: (i) a 3D plot using all calculated angle values of $\varphi 4$ and (ii) a 2D plot using three angle values of $\varphi 4$, 180° (squares), 60° (circles), and −60° (triangles), as found in **STATE_1**, **STATE_2**, and **STATE_3**, respectively.

when compared with CP55244.[39] However, if the receptor binding space were such that both A and C rings of CP47497 could be held in space by the receptor residues in the same way as for the ACD-ring moiety of CP55244, then the affinity and/or efficacy of analogues of CP47497 would not be compromised.

Ligand Isomerization To Release the Ligand Strain Energy as the Driving Force for Receptor Conformational Change. We have made the assumption that the ligand in the ground-state receptor-bound conformation is not in the lowest energy form. Based on the present calculations, the structural strain imposed on CP55244 in the receptor-bound ground-state conformation tended to be released in such a way that rotation of the ligand overcomes low rotational energy barriers to allow the ligand to attain the lowest possible energy conformations. We propose that ligand conformational isomerization to relieve the strain energy, E_{strain}, in the ligand bound to the receptor would be the driving force for inducing receptor conformational changes necessary for transferring signal to G-proteins.

A complete description of the binding free energy (ΔG_{bind})[40] for the ligand and two different receptor conformations, R and R*, can be written as follows:

for the R conformation

$$\Delta G_{bind,R} = \Delta H_{bind,R} + \Delta H_{conform,R} - T(\Delta S_{transl,R} + \Delta S_{rot,R} + \Delta S_{flex,R}) + \Delta G_{solvation,R}$$

for the R* conformation

$$\Delta G_{bind,R^*} = \Delta H_{bind,R^*} + \Delta H_{conform,R^*} - T(\Delta S_{transl,R^*} + \Delta S_{rot,R^*} + \Delta S_{flex,R^*}) + \Delta G_{solvation,R^*}$$

where ΔH_{bind} is the intermolecular binding interaction energy (i.e., van der Waals and Coulombic); $\Delta H_{conform}$ is the intramolecular strain energy in the bound state; ΔS_{transl}, ΔS_{rot}, and ΔS_{flex} are the translational, rotational, and torsional degrees of freedom upon ligand binding; and $\Delta G_{solvation}$ is the solvation free energy.

The formation of the R*-ligand complex is known to be energetically favored over that of the R-ligand complex (i.e., $\Delta G_{bind,R^*} - \Delta G_{bind,R} < 0$). Because the receptor conformational change from R to R* occurs within the receptor binding pocket, geometrical degrees of freedom and contributions from solvent would not be noticeably altered. Thus, the contribution of ΔS (ΔS_{transl}, ΔS_{rot}, and ΔS_{flex}) and $\Delta G_{solvation}$ would be negligible. In addition, because the ligand forms a favorable intermolecular binding interaction whether it fits into R or induces R* to fit, $\Delta H_{bind,R^*}$ appears to be roughly the same as $\Delta H_{bind,R}$. Overall, the energy required for the ligand-initiated induction of R* from R is stored in the form of $\Delta H_{conform}$, which would be the driving force for inducing R* as a result of releasing unfavorable structural strain imposed on the ligand.

Our present calculations showed that the C3 side chain of the receptor-bound conformation of CP55244 was in a highly constrained state (**STATE_1**) and prone to release its internally constrained energy (~5−6 kcal/mol, Table 1) by changing the C3 side chain orientation to a low energy unconstrained state (**STATE_2**, **STATE_3**, or **STATE_4**). The major contributors to this decrease in E_{total} could be attributed to torsion and van der Waals, while electrostatic interactions exhibited a relatively smaller opposing energy change (Table 1). This ligand conversion would be able to induce a receptor conformational change without requiring a significant external energy source. We identified those rotatable bonds of CP55244 as the combined torsion angles $\varphi 1$ and $\varphi 4$. It was estimated that the rotational barriers for this conversion orchestrated by $\varphi 1$ and $\varphi 4$ in CP55244 and CP47497 were acceptably low (<5 kcal/mol).

Table 1. Comparison of the Ground-State Receptor-Bound Conformation **STATE_1**[a] of CP55244 Determined from a Previous Docking Study[29] with the Low Energy Conformations **STATE_2**,[b] **STATE_3**,[b] and **STATE_4**[b] of CP55244 Identified from the 35 ns MD Simulation

	STATE_1	STATE_2	STATE_3	STATE_4
	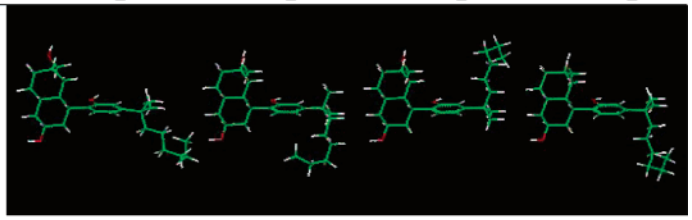			
torsion angles, degree				
φ1(C2-C3-C1'-C2')	*114 (107)*[c]	*56*	*–56*	*124*
φ2(C1-C6-C7-C16)	115 (123)[c]	120	119	120
φ3(C13-C14-C17-O)	62 (61)[c]	61	61	61
φ4(C3-C1'-C2'-C3')	*173 (180)*[c]	*61*	*–61*	*–61*
φ5(C1'-C2'-C3'-C4')[d]	–176 (–179)[c]	–176	178	178
φ6(C2'-C3'-C4'-C5')[d]	– 179 (180)[c]	178	180	180
φ7(C3'-C4'-C5'-C6')[d]	–98 (–97)[c]	–96	–96	–97
φ8(C4'-C5'-C6'-C7')[d]	64 (64)[c]	64	64	64
energy components, kcal/mol				
stretch	8.14 (9.27)[c]	9.10	9.11	9.12
bend	10.73 (9.59)[c]	9.58	9.67	9.63
torsion	–2.30 (–4.10)[c]	–4.62	–4.65	–4.65
stretch-bend	0.84 (0.87)[c]	0.80	0.80	0.83
out-of-plane	0.07 (0.01)[c]	0.00	0.00	0.00
1-4 van der Waals	55.56 (53.71)[c]	53.63	53.59	53.59
van der Waals	2.81 (2.54)[c]	1.63	1.84	1.98
1-4 electrostatic	–1.99 (–1.99)[c]	–1.98	–1.98	–1.99
electrostatic	1.18 (1.21)[c]	1.20	1.20	1.21
E_{total}	75.04 (71.10)[c]	69.34[e]	69.58[e]	69.72[e]
$E_{relative}$	0.00	–5.70	–5.46	–5.32

[a] To obtain **STATE_1**, the CB_1 receptor-CP55244 docking complex from our previous study by the CVFF force field[29] was fully energy minimized using the MMFF94 force field. Only receptor residues within 6 Å of CP55244 were included. Then, CP55244 was extracted and subjected to a single point energy calculation. [b] Fully energy minimized using the MMFF94 force field. [c] The value in parentheses was obtained after full energy minimization. [d] These torsion angles are assumed to remain unchanged. [e] The lowest possible energy conformation that was calculated from the conformational analysis (see the Computational Methods section) was 65.51 kcal/mol.

To examine how much the structural conversion of CP55244 from the receptor-bound conformation to the most stable and probable conformations, **STATE_2**, **STATE_3**, and **STATE_4**, would cause a steric clash within the CB_1 receptor pocket, $\varphi 1$ and $\varphi 4$ were rotated in the following different directions as shown in the 35 ns MD trajectory: one from 114° and 173° to 56° and 61° (**STATE_2**); the second from 114° and 173° to −56° and −61° (**STATE_3**); and the third from 114° and 173° to 124° and −61° (Figure 7). Starting from the binding conformation (**STATE_1**) that was previously determined by docking simulations,[29] the conversion to **STATE_2** or **STATE_4** produced a highly unfavorable steric interaction with TM3 of the receptor. The conversion to **STATE_3** produced a highly unfavorable steric interaction with TM6 of the receptor. Thus, these ligand conversions, through the repositioning of the C3 side chain of CP55244, could be proposed to induce receptor micro-conformational changes required for G-protein activation.

DISCUSSION

Molecular Mechanism of CP55244-Induced CB_1 Receptor Conformational Change. We hypothesize that a ligand conformational change, induced by rotating around $\varphi 1$ and $\varphi 4$ of CP55244, allows the C3 side chain to trigger a receptor conformational change. This receptor conformational change could be a major driving force leading to G-protein activation.

i. The ACD-Ring Moiety as the Plug for Ligand Rotation. The molecular mechanism of rhodopsin's activation begins with the docking of the ligand such that the protonated Schiff base forms a covalent bond that would serve as the plug. This is followed by the photoisomerization step of 11-*cis*-retinal to the all-*trans* form as a key step for ensuring the conversion of the light energy into the strain energy. The conformational change in the ligand is a requisite step for the conformational change in the receptor.[41−43] Although diffusible ligands are unable to form a covalent bond for the function of stabilizing the plug, it can be envisioned that reasonably high affinity, reversible, non-covalent interactions would function as the plug for these receptors. Classical and nonclassical cannabinoid ligands possess several pharmacophoric points of ligand−receptor interaction. The A-ring OH has been proposed to interact with the critical K3.28(192)[44,45] and, when present in this series of ligands, the C-ring OH and the D-ring OH can serve as additional pharmacophoric elements.[46] From our docking study of nonclassical cannabinoids,[29] the A-ring OH formed a hydrogen bonding network with K3.28(192) and E(258) in the human or K(259) in the rodent receptors. The D-ring OH formed a hydrogen bond with Q(261), and the hydrophobic ACD-ring was important for enhancing the binding via interactions with F2.61(174), L3.29(193), T3.37(201), F7.35(379), S7.39(383), and L7.43(387). The interaction between the D-ring and its hydroxyl group with the receptor would be strong enough (∼10 kcal/mol)[29] to prevent the D-ring hydroxyl group from the flip-flop depicted as a possible conversion of $\varphi 3$ (Figure 4). It was shown from the MD simulation that $\varphi 2$ remained unchanged around the

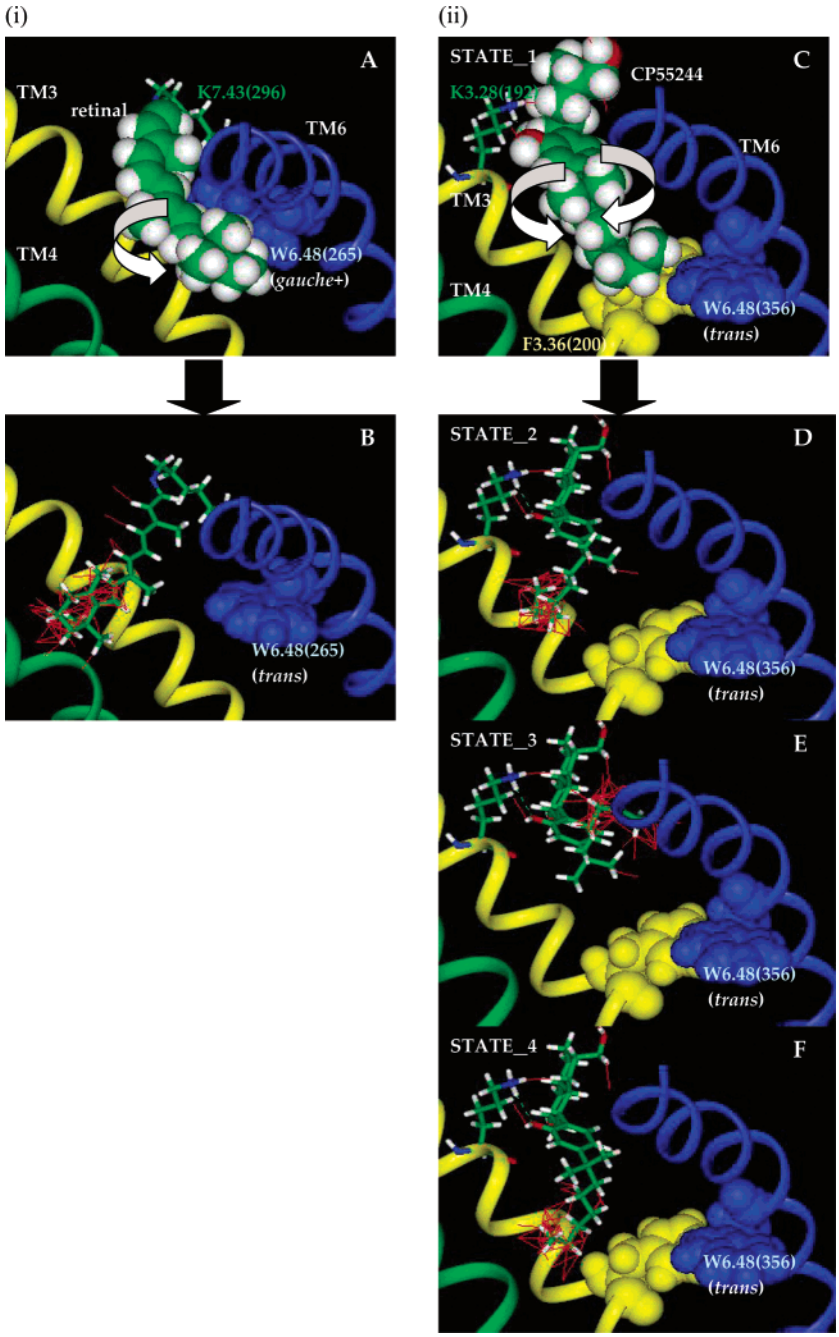

Figure 7. GPCR activation mechanisms for rhodopsin (panels A and B) and for the CB_1 receptor (panels C−F). For rhodopsin, retinal (in space-filling depiction in panel A and in stick depiction in panel B) is shown docked into rhodopsin as determined by X-ray crystallography.[19] A. 11-*cis* Retinal is covalently bound to TM7 K7.43(296) (in stick depiction) as the protonated Schiff base. B. The β-ionone ring moiety of retinal functions as the steric trigger for inducing a rhodopsin microconformational change in this depiction of the steric clash between the all-*trans* form of retinal and TM3/TM4 of rhodopsin. By the photoisomerization of the ligand, the rotamer toggle switch W6.48(265) (in space-filling depiction and in blue) would modulate the proline kink (see text). For the CB_1 receptor, CP55244 (in space-filling depiction in panel C and in stick depiction in panels D−F). C. The ground-state CB_1 receptor as **STATE__1**, as determined previously,[29] is participating in a hydrogen bonding interaction (in green dots) between the phenolic hydroxyl of CP55244 and TM3 K3.28(192) (in stick depiction). D−F. The C3 side chain of CP55244 functions as the steric trigger for inducing a CB_1 receptor conformational change: steric interference between **STATE__2** of CP55244 and TM3 of the CB_1 receptor (panel D); steric interference between **STATE__3** of CP55244 and TM6 of the CB_1 receptor (panel E); and steric interference between **STATE__4** of CP55244 and TM3 of the CB_1 receptor (panel F). By ligand binding and/or ligand structural modification, the rotamer toggle switch W6.48(265) (in space-filling depiction and in blue) and F3.36(200) (in space-filling depiction and in yellow) would be able to modulate the receptor microconformation (see text). TM3, TM4, and TM6 are colored in yellow, green, and blue, respectively. Color coding of retinal, CP55244, K7.43(296), and K3.28(192): green, C; red, O; and white, H.

value of 120°, suggesting that the A-ring connection to the C/D-ring would be rigidly fixed in space and would not participate as a movable component in a ligand−receptor conformational change. These nonbonding interactions would be important for securing the ACD-ring in place to serve as the plug.

ii. The C3 Side Chain of Cannabinoid Agonists as the Steric Trigger for Receptor Conformational Change. As

envisioned for rhodopsin, upon photoactivation of retinal, the salt bridge between E6.30(247) and the TM3 ERY motif of rhodopsin would be cleaved,[47] and the cytoplasmic region of TM7 would move away from the TM core region.[48] A recent cross-linking experiment indicated that the β-ionone ring of retinal was close to W6.48(265) of rhodopsin in the dark, as proved from the X-ray rhodopsin structure,[19] but was close to A4.58(169) in TM4 in the light.[42] These observations suggest that the 11-*cis* to all-*trans* ligand isomerization accompanied by repositioning of the β-ionone ring of retinal is the steric trigger which would disrupt the binding environment and rearrange the surrounding helices, especially TM3 through TM6 of rhodopsin.[14,22]

Contrary to the case with rhodopsin, the CB_1 receptor has no external energy available for the bound ligand to induce a receptor conformational change. We propose that the C3 side chain can serve as the steric trigger as the result of release of ground-state receptor binding constraints around the $\varphi 1$ and $\varphi 4$ torsion angles. Compared with the very high rotational energy barriers (35 kcal/mol) of retinal for rhodopsin activation,[49] it is likely that rotational energy barriers ($\sim$5 kcal/mol, Figure 2) of the C3 side chain moiety of CP55244 may cause a significant change in the receptor hydrophobic pocket, composed of residues mainly from TM3 and TM6. We envision that the change in orientation of the C3 side chain creates an unfavorable steric clash with the receptor hydrophobic pocket and disrupts the critical interaction with the neighboring helices, leading to receptor conformational change.

It is of particular interest that the ligand movements reported here have the potential to alter the CB_1 receptor TM3 and/or TM6. It has been proposed that for rhodopsin-like GPCRs, an ionic lock comprising the highly conserved E/DRY sequence along the intracellular side of TM3 with an E/D at the intracellular side of TM6 maintains the receptor in its ground-state conformation.[6,14,16,50−52] Agonist activation has been proposed to occur via interaction with amino acid residues surrounding the proline kink in TM6, which would trigger either rotation, movement of the intracellular side of the helix using the proline as a "flexible hinge", or helical tilting of TM6 using the proline as a lever, thereby disrupting the conformationally restricting interaction of TM3 and TM6 at the membrane surface.[50,51,53−55] Although it is unclear exactly how this helical movement occurs, or whether movement is identical for all GPCRs, the ultimate modification in the intracellular loop 3 interaction with the G-protein provides a mechanism for G-protein activation.

Observing in the X-ray structure of ground-state rhodopsin that the β-ionone ring and the carbon chain of retinal stabilize W6.48(265) of rhodopsin in the *gauche*+ rotamer conformation,[19] Shi and colleagues[55] proposed a β_2 adrenergic receptor activation mechanism. Thus, an inverse agonist stabilizes W6.48(265) and F6.52(290) both in their *gauche*+ rotamer conformations, while an agonist stabilizes F6.52(290) in its *trans* rotamer conformation and frees W6.48(286) in its *trans* rotamer conformation for the receptor activation. Adopting this rotamer toggle switch mechanism[55] to the CB_1 receptor, Reggio's group studied the CB_1 TM6 using a biased Monte Carlo Conformational Memories method[56] to analyze the peptide conformation in the absence of the surrounding receptor structure. They demonstrated that a *gauche*+ to *trans* transition of W6.48(356) (within the TM6 CWxP sequence) was associated with an increased probability of a straightening of the helix kink at P6.50(358).[56] From those studies, it was proposed that the inactive state of the CB_1 receptor would be associated with an interaction of TM3 F3.36 in its *trans* form and TM6 W6.48(356) in its *gauche*+ form, and the activated state would be associated with a coordinated rotameric transition to F3.36(200) in its *gauche*+ and W6.48(356) in its *trans* conformers.[56] However, no description was provided in their study regarding how the ligand could regulate this rotamer toggle switch.

In their effort to understand the role of cannabinoid ligands on CB_1 receptor activation, Reggio's group proposed another mechanism by which the alkyl side chain of cannabinoid agonists would fit into a VxxI helical groove just proximal to the CWxP sequence.[57] To explore this possibility using the Conformational Memories methods, they docked a pentane molecule (representing the alkyl side chain of Δ^9-THC) into this groove in the isolated CB_1 TM6 helix peptide and found an increased probability of helical conformations in the less-kinked (straighter) form. Straightening of the TM6 was proposed to destabilize the TM3 DRY-TM6 D ionic bridge that is believed to be one mechanism to maintain GPCRs in the ground state.

In the present investigation, we have sought to explore the mechanism by which the agonist can plug into the receptor in the ground state and subsequently provide the activation energy for the protein to achieve a higher energy activated state. In our analysis, the alkyl side chain is able to adopt three conformational positions that are lower in energy than the position proposed for the agonist as it would initially interact with the ground-state receptor. As these movements occur, the receptor must adjust accordingly. By examining the steric hindrances that are evident as the ligand is transformed to one or more of its lowest free energy states, we can predict the modifications in the helices that alter ground-state conformations of TM3, TM6, or both (Figure 7). Thus, our studies suggest that the ligand could exist in more than one conformationally distinct, lowest free energy state and induce a series of receptor microconformations. This is consistent with protein ensemble theory describing proteins as a collection of conformational states.[58] One potential conformation may exist in which the alkyl side chain nestles into a hydrophobic groove as predicted by Reggio's group,[57] and several potential "grooves" are available into which a pentane-like chain could bind. In our receptor model, the alkyl side chain of CP55244 is not able to fit into the VxxI helical groove because this region is located some distance from the receptor core region. Instead, the end of the alkyl side chain of CP55244 initially interacts with F3.36(200) and W6.48(356) in the ground-state receptor, and additional interactions secure the agonist with residues in TM2, TM3, and the extracellular loop 2 (Figure 7).[29] The side chain interactions with F3.36(200) and W6.48(356), though not major for the side chain,[29] are consistent with what Reggio's group proposed as the rotamer toggle switch.[56] These interactions would become no longer viable as the agonist side chain flips into lower energy positions, and this might be sufficient to free F3.36(200) and/or W6.48(356) to modulate the proline kink for the receptor activation.[55] It is interesting to notice in the present docking model that F3.36(200) and W6.48(356) exist in the *trans* conformations. This is consistent with the notion of Shi and colleagues that

the presence of the diffusible agonist stabilizes F6.52(290) and W6.48(286) of the β_2 adrenergic receptor in their *trans* rotamer conformations.[55] Thus, according to our docking model, the ligand would play an important role in turning on a potential rotamer switch F3.36(200) and/or W6.48(356) of the ground-state receptor. The ligand, then, changes its conformation in order to induce the receptor microconformational change.

Our studies demonstrate that the alkyl side chain of cannabinoid agonists can modify the microconformation of TM3 and/or TM6. In Figure 7, the possible molecular mechanism of the CB_1 receptor activation is compared with that of rhodopsin. For rhodopsin, light-activated isomerization of the β-ionone ring moiety of retinal causes a significant steric clash with TM3 and TM4, leading to the receptor conformational change. The rotamer switch W6.48(265) of rhodopsin, on the other hand, would be freed to modulate the proline kink for the receptor activation.[55] For the CB_1 receptor, we propose that the change in orientation of the C3 side chain would create an unfavorable steric clash with the receptor hydrophobic pocket, not only with TM3 (by **STATE_2** and **STATE_4**) but also with TM6 (by **STATE_3**) (Figure 7). Microconformational changes induced as a result could disrupt the critical interaction between the neighboring helices that would maintain the ground-state of the receptor.

CONCLUSIONS

In summary, using the CB_1 receptor as a study tool, we have proposed a molecular mechanism for the ligand-induced GPCR receptor conformational change. This is based on the premise that the initial binding conformation to which the ligand conforms in the ground state of the receptor is not the lowest energy that the ligand can achieve. As the ligand undergoes structural modifications that approach the lowest energy conformations, the development of steric clashes with the protein structure provides the energy necessary to overcome thermodynamic barriers to microconformational changes in the receptor. This mechanism would suggest that rotational flexibility in a ligand may be as important a determinant of agonist activity as the pharmacophoric elements that can be identified.

ACKNOWLEDGMENT

We wish to thank the National Institute on Drug Abuse for support for this work via grants R01-DA06312, R01-DA03690, K05-DA00182, and U24-DA12385.

REFERENCES AND NOTES

(1) Ji, T. H.; Grossmann, M.; Ji, I. G Protein-Coupled Receptors. *J. Biol. Chem.* **1998**, *273*, 17299−17302.
(2) Gether, U. Uncovering Molecular Mechanisms Involved in Activation of G Protein Coupled Receptors. *Endocr. Rev.* **2000**, *21*, 90−113.
(3) Drews, J. Drug Discovery: A Historical Prospective. *Science* **2002**, *287*, 1960−1964.
(4) Probst, W. C.; Snyder, L. A.; Schuster, D. I.; Brosius, J.; Sealfon, S. C. Sequence Alignment of the G-Protein Coupled Receptor Superfamily. *DNA Cell. Biol.* **1992**, *11*, 1−20.
(5) Ballesteros, J. A.; Weinstein, H. In *Methods in Neuroscience*; Conn, P. M., Sealfon, S. C., Eds.; Academic Press: San Francisco, 1995; Vol. 25, Chapter 19, pp 366−428.
(6) Ballesteros, J. A.; Jensen, A. D.; Liapakis, G.; Rasmussen, S. G.; Shi, L.; Gether, U.; Javitch, J. A. Activation of the β_2-Adrenergic Receptor Involves Disruption of an Ionic Lock between the Cytoplasmic Ends of Transmembrane Segments 3 and 6. *J. Biol. Chem.* **2001**, *276*, 29171−29177.
(7) Iiri, T.; Farfel, Z.; Bourne, H. R. G-Protein Diseases Furnish a Model for the Turn-On Switch. *Nature* **1998**, *394*, 35−38.
(8) Samama, P.; Cotecchia, S.; Costa, T.; Lefkowitz, R. J. A Mutation-Induced Activated State of the β_2-Adrenergic Receptor. Extending the Ternary Complex Model. *J. Biol. Chem.* **1993**, *268*, 4625−4636.
(9) Colquhoun, D. Binding, Gating, Affinity and Efficacy: the Interpretation of Structure−Activity Relationships for Agonists and of the Effects of Mutating Receptors. *Br. J. Pharmacol.* **1998**, *125*, 924−947.
(10) Bennett, W. S., Jr.; Steitz, T. A. Glucose-induced Conformational Change in Yeast Hexokinase. *Proc. Natl. Acad. Sci. U.S.A.* **1978**, *75*, 4848−4852.
(11) Gether, U.; Lin, S.; Kobilka, B. K. Fluorescent Labeling of Purified β_2 adrenergic Receptor. Evidence for Ligand-specific Conformational Changes. *J. Biol. Chem.* **1995**, *270*, 28268−28275.
(12) Waelbroeck, M. Kinetics versus Equilibrium: the Importance of GTP in GPCR Activation. *Trends. Pharmacol. Sci.* **1999**, *20*, 477−481.
(13) Natochin, M.; Moussaif, M.; Artemyev, N. O. Probing the Mechanism of Rhodopsin-catalyzed Transducin Activation. *J. Neurochem.* **2001**, *77*, 202−210.
(14) Farrens, D. L.; Altenbach, C.; Yang, K.; Hubbell, W. L.; Khorana, H. G. Requirement of Rigid-body Motion of Transmembrane Helices for Light Activation of Rhodopsin. *Science* **1996**, *274*, 768−770.
(15) Gether, U.; Kobilka, B. K. G Protein-coupled Receptors. II. Mechanism of Agonist Activation. *J. Biol. Chem.* **1998**, *273*, 17979−17982.
(16) Ghanouni, P.; Steenhuis, J. J.; Farrens, D. L.; Kobilka, B. K. Agonist-induced Conformational Changes in the G-protein-coupling Domain of the β_2 Adrenergic Receptor. *Proc. Natl. Acad. Sci. U.S.A.* **2001**, *98*, 5997−6002.
(17) Warshel, A. Bicycle-pedal Model for the First Step in the Vision Process. *Nature* **1976**, *260*, 679−683.
(18) Shieh, T.; Han, M.; Sakmar, T. P.; Smith, S. O. The Steric Trigger in Rhodopsin Activation. *J. Mol. Biol.* **1997**, *269*, 373−384.
(19) Palczewski, K.; Kumasaka, T.; Hori, T.; Behnke, C. A.; Motoshima, H.; Fox, B. A.; Le Trong, I.; Teller, D. C.; Okada, T.; Stenkamp, R. E.; Yamamoto, M.; Miyano, M. Crystal Structure of Rhodopsin: A G protein-coupled Receptor. *Science* **2000**, *289*, 739−745.
(20) Meyer, C. K.; Bohme, M.; Ockenfels, A.; Gartner, W.; Hofmann, K. P.; Ernst, O. P. Signaling States of Rhodopsin. *J. Biol. Chem.* **2000**, *275*, 19713−19718.
(21) Vogel, R.; Fan, G. B.; Sheves, M.; Siebert, F. *Biochemistry* **2000**, *39*, 8895−8908.
(22) Röhrig, U. F.; Guidoni, L.; Rothlisberger, U. Early Steps of the Intramolecular Signal Transduction in Rhodopsin Explored by Molecular Dynamics Simulations. *Biochemistry* **2002**, *41*, 10799−10809.
(23) Meng, E. C.; Bourne, H. R. Receptor Activation: What Does the Rhodopsin Structure Tell Us? *Trends Pharmacol. Sci.* **2001**, *22*, 587−593.
(24) Sakmar, T. P.; Menon, S. T.; Marin, E. P.; Awad, E. S. RHODOPSIN: Insights from Recent Structural Studies. *Annu. Rev. Biophys. Biomol. Struct.* **2002**, *31*, 443−484.
(25) Schoenlein, R. W.; Peteanu, L. A.; Mathies, R. A.; Shank, C. V. The First Step in Vision: Femtosecond Isomerization of Rhodopsin. *Science* **1991**, *254*, 412−415.
(26) Wang, Q.; Schoenlein, R. W.; Peteanu, L. A., Mathies, R. A.; Shank, C. V. Vibrationally Coherent Photochemistry in the Femtosecond Primary Event of Vision. *Science* **1994**, *266*, 422−4224.
(27) Devane, W. A.; Dysarz, F. A., III.; Johnson, M. R.; Melvin, L. S.; Howlett, A. C. Determination and Characterization of a Cannabinoid Receptor in Rat Brain. *Mol. Pharmacol.* **1988**, *34*, 605−613.
(28) Howlett, A. C.; Fleming, R. Cannabinoid Inhibition of Adenylate Cyclase. Pharmacology of the Response in Neuroblastoma Cell Membranes. *Mol. Pharmacol.* **1984**, *26*, 532−538.
(29) Shim, J.-Y.; Welsh, W. J.; Howlett, A. C. Homology Model of the CB_1 Cannabinoid Receptor: Sites Critical Nonclassical Cannabinoid Agonist Interaction. *Biopolymers (Peptide Science)* **2003**, *71*, 169−189.
(30) Halgren, T. A. Merck Molecular Force Field. I. Basis, Form, Scope, Parametrization, and Performance of MMFF94. *J. Comput. Chem.* **1996**, *17*, 490−519.
(31) Dewar, M. J. S.; Zoebisch, E. G.; Healy, E. F.; Stewart, J. J. P. AM1: A New General Purpose Quantum Mechanical Molecular Model. *J. Am. Chem. Soc.* **1985**, *107*, 3902−3909.
(32) Hehre, W. J.; Radom, L.; Schleyer, P. v. R.; Pople, J. A. *Ab Initio Molecular Orbital Theory*; Wiley: New York, 1986.
(33) *Density functional methods in chemistry*; Labanowski, J. K., Andzelm, J. W., Eds.; Springer-Verlag: New York, 1991.
(34) Tao, Q.; McAllister, S. D.; Andreassi, J.; Nowell, K. W.; Cabral, G. A.; Hurst, D. P.; Bachtel, K.; Ekman, M. C.; Reggio, P. H.; Abood, M. E. Role of a Conserved Lysine Residue in the Peripheral Cannabinoid Receptor (CB_2): Evidence for Subtype Specificity. *Mol. Pharmacol.* **1999**, *55*, 605−613.

(35) Swope, W. C.; Andersen, H. C.; Berens, P. H.; Wilson, K. R. A Computer Simulation Method for the Calculation of Equilibrium Constants for the Formation of Physical Clusters of Molecules: Application to Small Water Clusters. *J. Chem. Phys*. **1982**, *76*, 637−649.
(36) Tuckerman, M.; Berne, B. J.; Martyna, G. J. Reversible Multiple Time Scale Molecular Dynamics. *J. Chem. Phys.* **1992**, *97*, 1990−2001.
(37) Martin, B. R.; Jefferson, R.; Winckler, R.; Wiley: J. L.; Huffman, J. W.; Crocker, P. J.; Saha, B.; Razdan, R. K. Manipulation of the Tetrahydrocannabinol Side Chain Delineates Agonists, Partial Agonists, and Antagonists. *J. Pharmacol. Exp. Ther.* **1999**, *290*, 1065−1079.
(38) Razdan, R. K.; Dalzel, H. C. Drugs Derived from Cannabinoids. 6. Synthesis of Cyclic Analogues of Dimethylheptylpyran. *J. Med. Chem.* **1976**, *19*, 719−721.
(39) Melvin, L. S.; Milne, G. M.; Johnson, M. R.; Subramaniam, B.; Wilken, G. H.; Howlett, A. C. Structure−activity Relationships for Cannabinoid Receptor-binding and Analgesic Activity: Studies of Bicyclic Cannabinoid Analogs. *Mol. Pharmacol*. **1993**, *44*, 1008−1015.
(40) von der Lieth, C.-W.; Kozar, T. Towards a Better Semiquantitative Estimation of Binding Constants: Molecular Dynamics Exploration of the Conformational Behaviour of Isolated Sialyllactose and Sialyllactose Complexed with Influenza A Hemagglutinin. *J. Mol. Struct. (THEOCHEM)* **1996**, *368*, 213−222.
(41) Jang, G. F.; Kuksa, V.; Filipek, S.; Barthl, F.; Ritter, E.; Gelb, M. H.; Hofmann, K. P.; Palczewski, K. Mechanism of Rhodopsin Activation as Examined with Ring-Constrained Retinal Analogues and the Crystal Structure of the Ground-State Protein. *J. Biol. Chem*. **2001**, *276*, 26148−26153.
(42) Borhan, B.; Souto, M.; Imai, H.; Shichida, Y.; Nakanishi, K. Movement of Retinal along the Visual Transduction Path. *Science* **2000**, *288*, 2209−2212.
(43) Pan, D.; Mathies, R. A. Chromophore Structure in Lumirhodopsin and Metarhodopsin I by Time-Resolved Resonance Raman Microchip Spectroscopy. *Biochemistry* **2001**, *40*, 7929−7936.
(44) Song, Z.-H.; Bonner, T. I. A Lysine Residue of the Cannabinoid Receptor Is Critical for Receptor Recognition by Several Agonists but Not WIN55212-2. *Mol. Pharmacol.* **1996**, *49*, 891−895.
(45) Chin, C.; Abadji, V.; Lucas-Lenard, J.; Kendall, D. Ligand Binding and Modulation of Cyclic AMP Levels Depends on the Chemical Nature of the Residue 192 of the Human Cannabinoid Receptor 1. *J. Neurochem*. **1998**, *70*, 366−373.
(46) Howlett, A. C.; Johnson, M. R.; Melvin, L. S.; Milne, G. M. Nonclassical Cannabinoid Analgetics Inhibit Adenylate Cyclase: Development of a Cannabinoid Receptor Model. *Mol. Pharmacol*. **1988**, *33*, 297−302.
(47) Arnis, S.; Fahmy, K.; Hofmann, K. P.; Sakmar, T. P. A Conserved Carboxylic Acid Group Mediates Light-Dependent Proton Uptake and Signaling by Rhodopsin. *J. Biol. Chem.* **1994**, *269*, 23879−23881.
(48) Altenbach, C.; Cai, K.; Klein-Seetharaman, J.; Khorana, H. G.; Hubbell, W. L. Structure and Function in Rhodopsin: Mapping Light-Dependent Changes in Distance between Residue 65 in Helix TM1 and Residues in the Sequence 306−319 at the Cytoplasmic End of Helix TM7 and in Helix H8. *Biochemistry* **2001**, *40*, 15483−15492.
(49) Saam, J.; Tajkhorshid, E.; Hayashi, S.; Schulten, K. Molecular Dynamics Investigation of Primary Photoinduced Events in the Activation of Rhodopsin. *Biophys. J.* **2002**, *83*, 3097−3112.
(50) Dunham, T. D.; Farrens, D. L. Conformational Changes in Rhodopsin. Movement of Helix F Detected by Site-Specific Chemical Labeling and Fluorescence Spectroscopy. *J. Biol. Chem.* **1999**, *274*, 1683−1690.
(51) Jensen, A. D.; Guarnieri, F.; Rasmussen, S. G.; Asmar, F.; Ballesteros, J. A.; Gether, U. Agonist-induced Conformational Changes at the Cytoplasmic Side of Transmembrane Segment 6 in the β_2-Adrenergic Receptor Mapped by Site-Selective Fluorescent Labeling. *J. Biol. Chem*. **2001**, *276*, 9279−9290.
(52) Greasley, P. J.; Fanelli, F.; Rossier, O.; Abuin, L.; Cotecchia, S. Mutagenesis and Modelling of the α_{1b}-Adrenergic Receptor Highlight the Role of the Helix 3/helix 6 Interface in Receptor Activation. *Mol. Pharmacol*. **2002**, *61*, 1025−1032.
(53) Lin, S. W.; Sakmar, T. P. Specific Tryptophan UV-absorbance Changes Are Probes of the Transition of Rhodopsin to its Active State. *Biochemistry* **1996**, *35*, 11149−11159.
(54) Liu, J.; Blin, N.; Conklin, B. R.; Wess, J. Molecular Mechanisms Involved in Muscarinic Acetylcholine Receptor-Mediated G Protein Activation Studied by Insertion Mutagenesis. *J. Biol. Chem*. **1996**, *271*, 6172−6178.
(55) Shi, L.; Liapakis, G.; Xu, R.; Guarnieri, F.; Ballesteros, J. A.; Javitch, J. A. β_2 Adrenergic Receptor Activation. Modulation of the Proline Kink in Transmembrane 6 by a Rotamer Toggle Switch. *J. Biol. Chem*. **2002**, *277*, 40989−40996.
(56) Singh, R.; Hurst, D. P.; Barnett-Norris, J.; Lynch, D. L.; Reggio, P. H.; Guarnieri, F. Activation of the Cannabinoid CB_1 Receptor May Involve a W6.48/F3.36 Rotamer Toggle Switch. *J. Pept. Res*. **2002**, *60*, 357−370.
(57) Barnett-Norris, J.; Hurst, D. P.; Lynch, D. L.; Guarnieri, F.; Makriyannis, A.; Reggio, P. H. Conformational Memories and the Endocannabinoid Binding Site at the Cannabinoid CB_1 Receptor. *J. Med. Chem*. **2002**, *45*, 3649−3659.
(58) Kenakin, T.; Onaran, O. The Ligand Paradox between Affinity and Efficacy: Can You Be There and Not Make a Difference? *Trends. Pharmacol. Sci.* **2002**, *23*, 275−280.

CI040040C